Microscopic evidence of $C40$ and $C54$ in $(Ti,Ta)Si_2$: Template mechanism

A. Mouroux,* T. Epicier,† S.-L. Zhang, and P. Pinard,‡
Department of Electronics, Royal Institute of Technology, Box E229, SE-164 40 Kista, Sweden
(Received 22 January 1999)

The formation of $C54$ $TiSi_2$ with a thin Ta layer deposited between Si and Ti is investigated at atomic scale level using transmission electron microscopy. When the Si/Ta/Ti structure is annealed at 650 °C for 30 s, both $C40$ and $C54$ $(Ti,Ta)Si_2$ are found at the Si/silicide interface. The Ta-to-Ti ratio in such $C40$ or $C54$ grains changes rapidly from 0.11–0.12 at the interface to 0 at a distance about 35 nm away from the interface. The observation of $C40$ $TiSi_2$ and $C54$ $(Ti_{0.89}Ta_{0.11})Si_2$, is a consequence of epitaxial growth at low temperatures. After annealing at 750 °C, the $C40$ phase is not detectable by electron or x-ray diffraction. These results verify, from a microscopic point of view, the template mechanism suggested earlier for the enhanced formation of $C54$ $TiSi_2$ in the presence of Mo, Nb, or Ta, based on the macroscopic analysis results. In addition, the high-Ta contents in the $C54$ phase induce a high concentration of stacking faults in the ⟨010⟩ direction along which epitaxy of $C54$ $(Ti,Ta)Si_2$ on $C40$ $(Ti,Ta)Si_2$ takes place. [S0163-1829(99)08535-5]

I. INTRODUCTION

Titanium disilicide ($TiSi_2$) can exist[1,2] in two different crystallographic phases: $C49$ and $C54$. It has been established[3–8] that the addition of a small amount of Mo, W, Nb, or Ta to the Ti-Si system enhances the formation of the $C54$ phase of $TiSi_2$ desirable for electronic device applications. Experimental observations,[9–12] supported by theoretical calculations,[13] show that the stable phase in ''$TiSi_2$'' shifts successively from $C49$ to $C54$ and then to $C40$ as the electron-to-atom (e/a) ratio increases. Replacing Ti with those four refractory metals[9] or substituting Sb for Si (Ref. [11]) results in an increased e/a ratio, while Sc in place of Ti (Ref. 10) or Al replacing Si (Ref. 12) leads to a decreased e/a ratio. In view of the great structural similarities between the $C40$ and $C54$ phases,[14] the enhanced formation of $C54$ $TiSi_2$ in the presence of the refractory metals has been attributed[4,6–8] to a template mechanism with the formation of a ternary $(Ti,RM)Si_2$ alloy of the $C40$ structure that leads to the direct growth of $C54$ $TiSi_2$. Cross-sectional transmission electron microscopy (TEM) was used[6] to confirm the crystallographic orientations of the $C54$ $TiSi_2$ formed in the presence of an interposed Mo layer. However, the analysis techniques used so far have been mainly those that provide macroscopic information, i.e., x-ray diffraction (XRD), resistance measurement, and Rutherford backscattering spectrometry (RBS). It is the purpose of the present study to investigate at the atomic scale level how the template mechanism occurs during the formation of $C54$ $TiSi_2$ in the presence of a Ta interlayer between Ti and Si.

II. EXPERIMENT

Tantalum and Ti layers were deposited consecutively on ⟨100⟩ Si substrates in a dual source e-beam evaporation system. The thickness of the metal layers was 1.3 nm for Ta and 87 nm for Ti, according to RBS analysis. The samples were annealed at 650 or 750 °C for 30 s in N_2. The unreacted metal was removed using a selective wet etch. The details of the sample preparation procedure can be found elsewhere.[6]

Mechanical polishing followed by ion milling was used to prepare samples for high-resolution cross-sectional TEM (HRTEM) studies on a 2010F Joel microscope at 200 kV. The samples were thinned to about 20 nm in order to obtain high-quality images at the atomic scale. To improve the resolution, the microscope was equipped with a filament for field emission. In addition to diffraction studies, energy dispersive x-ray spectroscopy was employed for chemical analysis. For the latter analysis, three different probes were used: 0.5, 0.7, and 1 nm. Fast Fourier transform (FFT) were performed, on the HRTEM images, to determine the crystallographic structures. Diffraction patterns obtained by FFT and/or electron diffraction were analyzed using a simulation program[15] that could generate diffraction patterns corresponding to all phases possibly present in the samples, i.e., $C49$ $TiSi_2$, $C54$ $(Ti,Ta)Si_2$, $C40$ $(Ti,Ta)Si_2$, and metal-rich silicides.

III. RESULTS AND DISCUSSION

The results presented below mainly concern the sample annealed at 650 °C. The cross-sectional picture shown in Fig. 1(a) was taken from the area close to the Si/silicide interface. A portion of a silicide crystal of about 50 nm by 80 nm cross-sectional area is depicted. The FFT result of this particular crystal is presented in Fig. 1(b). The distances between the central spot and the two marked reflection spots as well as the angle between the two reflections are measured to 0.219, 0.239 nm, and 90°, respectively. The measured results compare well with the corresponding values for the reflections (003) and $(1\bar{2}0)$ of $C40$ $TaSi_2$:[15] 0.21902, 0.23923 nm, and 90 °. Thus, the FFT pattern is assigned to the $C40$ phase oriented along the [210] axis. The [001] axis of the crystal forms an angle of about 70° with the normal of the Si/silicide interface as well as the sample surface [see Fig. 1(a)]. The diffraction pattern shown in Fig. 1(c) was obtained when examining another $C40$ grain also in the interface region. The distances between the central spot and two marked reflection spots are 0.414 and 0.350 nm, and the angle between the two reflections is 148°. These results again compare well with the corresponding values for the reflections $(\bar{1}10)$ and

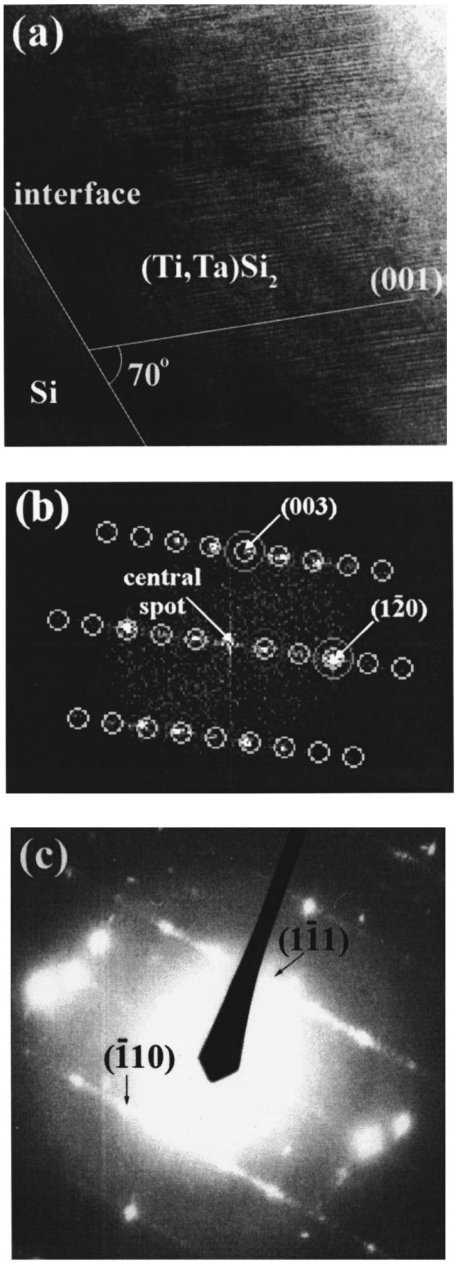

FIG. 1. Analysis of a $C40$ grain located close to the Si/silicide interface (a) its HRTEM image, and (b) its FFT result (bright spots), with the circles around being obtained by simulation, showing the grain along the zone axis [210]. In (c) a diffraction pattern was obtained on another $C40$ grain along the zone axis [110].

$(1\bar{1}1)$ of $C40$ $TaSi_2$: 0.4144, 0.3504 nm, and 147.8°. The pattern is assigned to the $C40$ phase oriented along the [110] axis. The (001) and (002) reflections should also appear in Fig. 1(c), according to dynamical theory. Intensity calculations indicate, however, that the two reflections are too weak to be detected because of the very thin sample used (about 20 nm).

Chemical analysis of the crystal shown in Fig. 1(a) revealed that the atomic ratio of Ta to Ti was about 0.11 at the Si/silicide interface and decreased rapidly when advancing deeper into the crystal away from the interface. Tantalum was not detectable already at a distance of about 35 nm from the interface, which is understandable as initially Ta was at

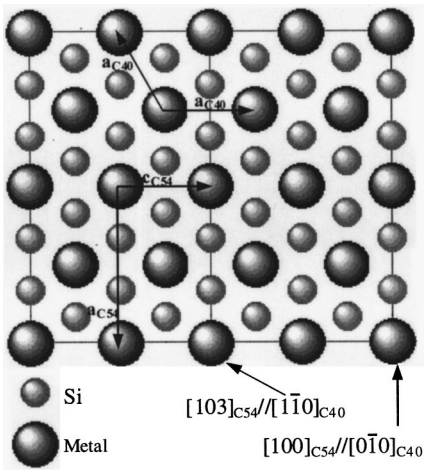

FIG. 2. Relationship between the [103] and [100] directions in the $C54$ structure and the $[1\bar{1}0]$ and $[0\bar{1}0]$ directions in the $C40$ structure.

the interface, and should remain immobile at 650 °C. Thus, the results in Fig. 1(a) clearly demonstrate the epitaxy of $C40$ $TiSi_2$ on $C40$ $(Ti,Ta)Si_2$. The phase diagram[16] of the $TiSi_2$-$TaSi_2$ binary system above 1200 °C shows that the minimum Ta-to-Ti ratio in $C40$ $(Ti,Ta)Si_2$ is about 0.5, i.e., $(Ti_{0.5}Ta_{0.5})Si_2$. A higher value of the ratio might be expected at 650 °C. Hence, the formation of $C40$ $(Ti,Ta)Si_2$ with low-Ta contents indicates that the system was far from thermodynamic equilibrium. The dominance of kinetic factors at 650 °C leads to the growth of the $C40$ $TiSi_2$; $TiSi_2$ normally exists in $C49$ and $C54$ structure.[1,2]

Numerous crystals in the $C54$ structure were identified whereas no grain in the $C49$ phase was detected in the silicide layer. The presence of Ta would hinder the formation of $C49$ $TiSi_2$, according to the theoretical calculations of Bonoli *et al.*[13] Most of the $C54$ crystals observed had an atomic structure homogeneous throughout the whole grain. The $C54$ crystals were oriented in such a way that their [010] axis formed an angle of about 70° with the sample surface normal. Therefore, the [010] axis of the $C54$ crystals was collinear with the [001] axis of the $C40$ crystal discussed above [Fig. 1(a)]; this is in accordance to the discussion in Ref. 6 for the $TiSi_2$ formation in the presence of a Mo interlayer. Because of the very small lattice mismatch (below 0.3%) between $C40$ $TaSi_2$ and $C54$ $TiSi_2$,[17] the basal $\langle 001 \rangle$ planes of the former structure is identical to the $\langle 010 \rangle$ planes of the latter. Figure 2 illustrates schematically how these two sets of planes are related: the directions [103] and [100] in the $C54$ structure are equivalent to the directions $[1\bar{1}0]$ and $[0\bar{1}0]$ in the $C40$ structure, respectively.

In several crystals of the $C54$ structure in the close vicinity of the Si/silicide interface, two different structural variants were observed inside a same grain, see the lattice image depicted in Fig. 3(a). The diffraction patterns corresponding to the two variants are shown in Figs. 3(b) and 3(c). Analyses of the patterns, with the assistance of FFT (results not shown), indicate that the $C54$ structure in variant 1 is oriented along the zone axis [103] and that in variant 2 along [100]. In variant 1, the two marked spots in Fig. 3(b) are assigned to the (040) (0.2138 nm) and $(\bar{3}11)$ (0.2302 nm)

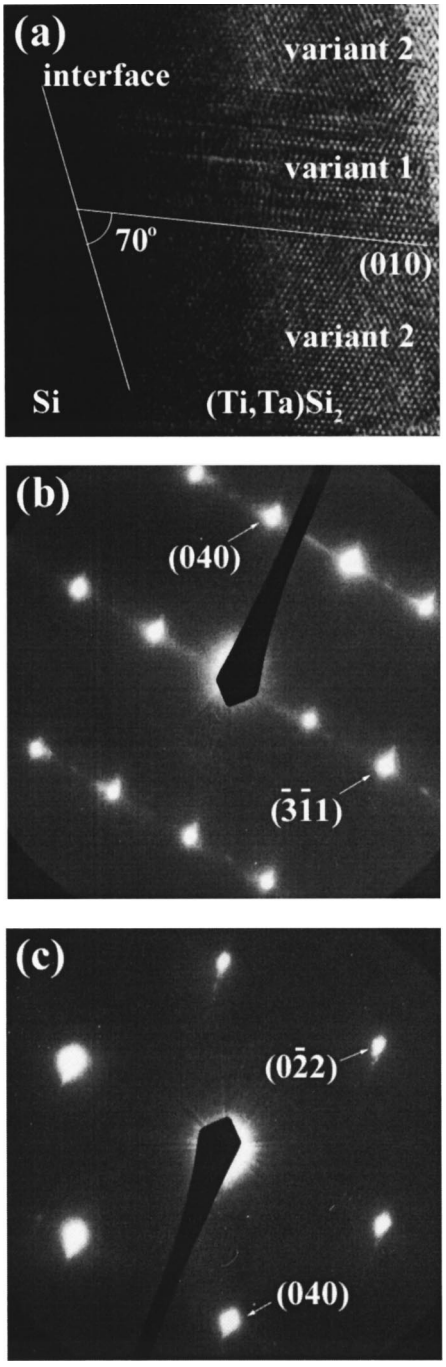

FIG. 3. Analysis of a $C54$ grain also located close to the Si/silicide interface (a) its HRTEM image showing two structural variants, as well as the diffraction patterns of (b) variant 1 along the zone axis [103] and (c) variant 2 along [100].

reflections that form an angle of 105.6° between them. In variant 2, the two marked spots in Fig. 3(c) are identified as the (040) (0.2138 nm) and $(0\bar{2}2)$ (0.2092 nm) reflections with an angle of 120° between them. What should be pointed out at this point is that those two variants of the $C54$ structure do share a common [010] crystallographic axis [Figs. 2 and 3(a)]. Once again, the absence of the allowed (020) reflection is attributed to the use of a too-thin sample.

The FFT analysis of variant 2 directly adjacent to the Si/silicide interface, where the sample was somewhat thicker, shows a different feature (Fig. 4) from the diffraction

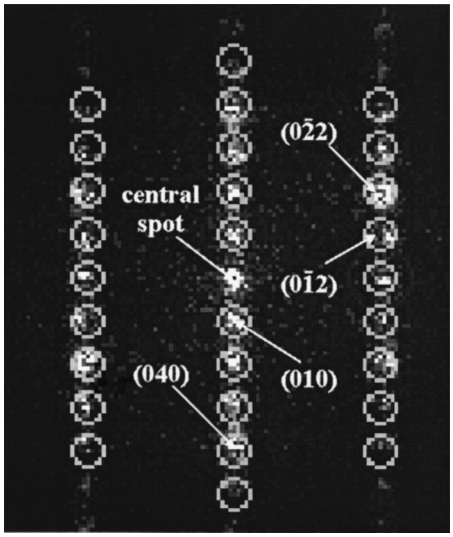

FIG. 4. FFT of variant 2 obtained directly adjacent to the Si/silicide interface in a slightly thicker area. The circles around the FFT spots are obtained by simulation.

result in Fig. 3(c). Additional spots are found at $\frac{1}{4}$ of the distance between the central spot and the spot corresponding to the (040) reflection, indicating the appearance of (010) reflection. The (010) reflection is, however, forbidden in the $C54$ structure according to dynamical theory. The substitution of Ta for Ti in the $C54$ structure (see below) may generate stacking faults, which has in fact been shown[18] to occur in a similar ternary system involving the interaction between Ta-W and Si. The presence of stacking faults can be responsible for the appearance of the (010) reflection. As a consequence, the $(0\bar{1}2)$ reflection also becomes visible (Fig. 4). The occurrence of stacking faults in the ⟨010⟩ direction is not surprising, since it is the direction along which planes of atoms arranged in hexagons are stacked in the *...ABCDA...* sequence to form the entire lattice of the $C54$ structure. It is also the axis along which the epitaxy of $C54$ on $C40$ takes place, because similar stacking yet in the *...ABCA...* sequence of hexagonal planes occurs along the ⟨001⟩ direction in the $C40$ structure.

The chemical analysis of the interfacial crystals with the $C54$ structure also showed a similar concentration gradient of Ta inside each grain, i.e., being higher at the Si/silicide interface and decaying rapidly with increasing distance to the interface. A difference was found between the two structural variants of the $C54$ structure; the Ta-to-Ti ratio at the interface was higher in variant 2 (0.12) than in variant 1 (0.05), though there was no Ta detectable in either variant far away from the interface. The high-temperature phase diagram[16] of $TiSi_2$-$TaSi_2$ shows that the solubility of Ta in $C54$ $TiSi_2$ is negligible. Therefore, the formation of $C54$ $(Ti,Ta)Si_2$ with measurable Ta contents also indicates that the system was in a nonequilibrium state.

Both $C40$ and $C54$ $(Ti,Ta)Si_2$ were found at the Si/silicide interface after annealing the Ti/Ta/Si structure at 650 °C. When the sample was annealed at 750 °C, the $C40$ $(Ti,Ta)Si_2$ disappeared and only $C54$ $(Ti,Ta)Si_2$ was detected by TEM in this work and by XRD in Ref. 6. The instability of the $C40$ structure has also been found in a similar system[19] with Ti-Nb alloyed films deposited on Si. When the Nb contents

in the alloy were below 10%, the $C40$ phase was always found prior to the $C54$ phase upon annealing from 100 to 1000 °C according to *in situ* XRD analysis. Therefore, it is suggested that the presence of Ta induced the formation of discrete $C40$ $(Ti,Ta)Si_2$ grains at the Si/Ti interface and prevented the formation of $C49$ $TiSi_2$. The existing nuclei of $C40$ $(Ti,Ta)Si_2$ led to the formation of $C54$ $(Ti,Ta)Si_2$ vertically as well as laterally throughout the layer. The growth of metastable $C54$ $(Ti,Ta)Si_2$ laterally at the Si/silicide interface, induced by the $C40$ $(Ti,Ta)Si_2$, could only be possible at low temperatures.

IV. CONCLUSIONS

Nonequilibrium disilicides $C40$ $TiSi_2$ and $C54$ $(Ti_{0.89}Ta_{0.11})Si_2$ have been identified in the silicide layer formed by annealing the Si/Ta/Ti structure at 650 °C. The existence of such nonequilibrium phases is a consequence of epitaxial growth at low temperatures. Stacking faults were found in the $C54$ grain along the ⟨010⟩ orientation. These observations verify, from a microscopic point of view, the template mechanism,[4,6–8] for the enhanced formation of $C54$ $TiSi_2$ in the presence of Mo, Ta, and Nb that was originally suggested on the basis of macroscopic results.

ACKNOWLEDGMENTS

B. Reynard is acknowledged for involvement in this project, and Professor F. M. d'Heurle is thanked for enlightening discussions. This work was partly supported by the Swedish Research Council for Engineering Sciences (TFR). A. M. was supported by the European Union (EU).

*Electronic address: aliette@ele.kth.se

†Present address: Laboratoire GEMPPM, UMR CNRS 5510, INSA de Lyon, F 69621 Villeurbanne, France.

‡Present address: Laboratoire de Physique de la Matière, UMR CNRS 5511, INSA de Lyon, F 69621 Villeurbanne, France.

[1] F. M. d'Heurle, P. Gas, I. Engström, S. Nygren, M. Östling, and C. S. Petersson, IBM Report No. 50067, 1985 (unpublished).

[2] R. Beyers and R. Sinclair, J. Appl. Phys. **57**, 5240 (1985).

[3] R. W. Mann, G. L. Miles, T. A. Knotts, D. W. Rakowski, L. A. Clevenger, J. M. E. Harper, F. M. d'Heurle, and C. Cabral, Jr., Appl. Phys. Lett. **67**, 3729 (1995).

[4] A. Mouroux, S.-L. Zhang, W. Kaplan, S. Nygren, M. Östling, and C. S. Petersson, Appl. Phys. Lett. **69**, 975 (1996).

[5] C. Cabral, Jr., L. A. Clevenger, J. M. E. Harper, F. M. d'Heurle, R. A. Roy, K. L. Saenger, G. L. Miles, and R. W. Mann, J. Mater. Res. **12**, 304 (1997).

[6] A. Mouroux, S.-L. Zhang, and C. S. Petersson, Phys. Rev. B **56**, 10 614 (1997).

[7] C. Cabral, Jr., L. A. Clevenger, J. M. E. Harper, F. M. d'Heurle, R. A. Roy, C. Lavoie, G. L. Miles, R. W. Mann, and J. S. Nakos, Appl. Phys. Lett. **71**, 3531 (1997).

[8] A. Mouroux, B. Reynard, and S.-L. Zhang, in *Advanced Metallization and Interconnect Systems for ULSI Applications in 1997*, edited by R. Cheung, J. Klein, K. Tsubouchi, M. Murakami, and N. Kobyashi (Materials Research Society, Warendale, PA, 1998), pp. 605–609.

[9] H. J. Goldschmidt, *Interstitial Alloys* (Butterworths, London, 1967), pp. 323–307 (now available from University Microfilms International, Ann Arbor, Michigan).

[10] O. Thomas, S. Delage, and F. M. d'Heurle, *Extended Abstracts*, (Electrochemical Society, Pennington, NJ, 1988), Vol. 88-1, p. 209.

[11] X.-H. Li, J. R. A. Carlsson, S. F. Gong, and H. T. G. Hentzell, J. Appl. Phys. **72**, 514 (1992).

[12] S.-L. Zhang, F. M. d'Heurle, C. Lavoie, C. Cabral, Jr., and J. M. E. Harper, Appl. Phys. Lett. **73**, 312 (1998).

[13] F. Bonoli, M. Iannuzzi, L. Miglio, and V. Meregalli, Appl. Phys. Lett. **73**, 1964 (1998).

[14] F. M. d'Heurle, in *VLSI Science and Technology*, edited by C. Dell'Oca and W. M. Bullis (The Electrochemical Society, Pennington, NJ, 1982), pp. 194–212.

[15] Standard JCPDS diffraction pattern 38-483 (hexagonal $TaSi_2$), JCPDS-International Center for Diffraction Data, PDF-2 Database, 12 Campus Boulevard, Newton Square, PA 19073-3273.

[16] H. Kudielka and H. Nowotny, Monatsch. Chem. **87/3**, 31 (1956).

[17] Standard JCPDS diffraction pattern 35-785 (orthorhombic $TiSi_2$), JCPDS-International Center for Diffraction Data, PDF-2 Database, 12 Campus Boulevard, Newton Square, PA 19073-3273.

[18] P. Gas, J. Tardy, F. K. LeGoues, and F. M. d'Heurle, J. Appl. Phys. **61**, 2203 (1987).

[19] A. Mouroux, M. Roux, S.-L. Zhang, J. M. E. Harper, F. M. d'Heurle, C. Cabral, Jr., and C. Lavoie (unpublished).